Progress In Electromagnetics Research, PIER 40, 229–254, 2003

RADIO WAVE PROPAGATION IN PERPENDICULAR STREETS OF URBAN STREET GRID FOR MICROCELLULAR COMMUNICATIONS. PART I: CHANNEL MODELING

H. M. El-Sallabi and P. Vainikainen

Radio Laboratory, Institute of Digital Communications
Helsinki University of Technology
Otakaari 5A, FIN-02015 HUT, Finland

Abstract—This paper proposes a spatial variant wideband propagation model for perpendicular street of urban street grid. Analytical expression of the spatial variant multi-ray channel transfer function is derived. The model provides characteristics of each ray in explicit expressions. The ray characteristics are given in terms of complex amplitude for both vertical and horizontal polarizations, path length, angle of arrival and departure. A set membership criteria is proposed to determine the coupling radio paths. The proposed model is not only capable in providing macroscopic quantities like mean field values and mean delay spread, but also the full wideband channel information, i.e., space dependent complex channel responses with a high time dispersion resolution. The proposed model can be used for studying different propagation problems in urban street grid for microcellular communications with applications e.g., antenna diversity techniques, multi-input multi-output (MIMO) channel capacity analysis, etc.

1. INTRODUCTION

The recent trend to increase the capacity of cellular systems has led to the adoption of the concept of microcells. The microcellular approach operating over short radio paths, using low antennas and low transmitting powers is expected to enhance the radio spectral density for future mobile communication systems. The antenna placement below rooftops results in propagation conditions that are dominated by multiple wall reflections [1], which are strongly affected by street structure and wall reflectivity, and diffraction at vertical edges of street corners [2]. The detailed characterization of the radio channel propagation is a major requirement for successful design of wireless communication systems. For this purpose, it is important to develop propagation models, which can predict propagation characteristics for microcellular environments.

To characterize the microcellular propagation, uniform geometrical theory of diffraction (UTD) [3, 4] and ray tracing techniques are often employed for theoretical propagation modeling of the two main physical processes: diffraction and reflection. Recently, ray-tracing techniques have been used for the prediction of multipath components in site-specific scenarios [6–13]. The ray tracing algorithms provide inherently the delays and the angles of arrival of multipath components, which are necessary information for future mobile communication systems utilizing adaptive antennas. Once all paths have been identified, high frequency electromagnetic techniques [3–5] such as UTD are applied to the rays to compute the amplitude, phase, delay, and polarization of each ray.

The lengthy time spent in ray-trace computation is a major existing problem with mobile radio propagation prediction for urban microcellular environments. This work, which is a continuation of our previous work [14], overcomes the computation time problem by developing propagation model in an explicit form expression. The advantage of a closed form model is the easiness in use for studying propagation problems such as the effect of a diffracting wedge, which may collapse the capacity of a multi-element MIMO arrays [15] since they may work as keyhole [16]. The explicit form expression provides the radio paths that couple the transmitter to the receiver at any point in the perpendicular street including paths having the same path length but different angle of arrival and departure. The proposed model is not only capable in providing macroscopic quantities like mean field values and mean delay spread, but also the full wideband channel information, i.e., space dependent complex channel responses with a high resolution in time dispersion. The proposed model is different from ray tracing

models in a sense that there is no searching for coupling radio paths between transmitter and receiver as ray characteristics are given in closed form.

The continuation of our previous work [14] is in terms of providing the model in an explicit expression and classifying the street grid in to three main parts, the line of sight street (called main street), which part is presented in [14] and perpendicular non-line of sight streets, which part is presented in this work, and parallel non-line of sight streets, which part is a subject of future work.

This paper, i.e., part I, presents channel model, part II will deal with channel characterization. The paper is organized as follows. In Section 2, analytical expression of the channel model is described in which are mathematical formulation for the different ray groups are given. Section 3 presents numerical results for validating the proposed model in terms of path gain, direction of arrival and path delay. Finally, the conclusions and recommendations of the paper are summarized in Section 4.

2. ANALYTICAL MODEL

Good knowledge of physical propagation mechanisms and channel behavior are important in developing an accurate propagation model. It is widely accepted that the main investigated propagation mechanisms in microcells are reflection and diffraction at vertical edges of street corners [1, 2, 6–13]. Therefore, in this model, two groups of rays are considered. The first group of rays is the reflection-reflection (*R*-*R*) rays group, which includes propagation paths via reflection along the main street and perpendicular street. The second group of rays is the reflected-diffracted-reflected (*R*-*D*-*R*) rays group, which consists of rays that may be reflected along the main street and diffracted at street corner and may be reflected again along the perpendicular street. In this work, we mean by main street as the street where the BS is located, the perpendicular street is the street branched from main street and where the MS is located, and the side streets are the branched streets between the BS and the perpendicular street. The rays are diffracted at all corners of the street junction between main and perpendicular streets. They may (or not) experience wall and (or not) ground reflections before and after diffraction. Image theory and horizontal plane angle set membership criteria are utilized to find the possible coupling paths. The method of images, combined with the uniform geometrical theory of diffraction, is a high-frequency approximation method, which has been applied to urban UHF propagation by many researchers [6–13]. The presented

model does not require reception tests, which makes it computationally faster. The height of antennas is assumed to be below the rooftops of the surrounding buildings, so rays diffracted over the building rooftops are neglected. It is assumed that the streets are flat, straight, and lined with tall buildings whose walls are assumed to be smooth flat surfaces with average complex relative permittivity (ε).

2.1. Channel Transfer Function

In order to simulate the behavior of data transmission through a medium under various conditions, it is essential to determine its transfer characteristics. Let $H(f, r)$ be the transfer function of a spatial variant multi-ray model, where f is the frequency and r is the path length. The total channel transfer function of the above mentioned propagation mechanism is given by

$$H_t = H_{RR} + H_{RDR} \tag{1}$$

where the H_{RR} and H_{RDR} are the total transfer functions of the *R-R* and the *R-D-R* ray groups, respectively. The following subsections present the derived expressions for calculating the transfer function of each group.

2.1.1. Reflection-Reflection Rays

The channel transfer function [14] of the *R-R* rays between the transmitting and the receiving antennas can be calculated by

$$H_{V,H} = \left(\frac{\lambda}{4\pi}\right) \sum_{i\equiv(m,S,n,u,g)} \left[f_B(\theta_i,\phi_i) f_M(\Theta_i,\Phi_i) \left(\Re^i_{V,H}\right)^g \left(R^{in}_{H,V}\right)^n \left(R^{im}_{H,V}\right)^m \frac{e^{-jkr_i}}{r_i} \right] \tag{2}$$

where a ray i is represented by a set of five integers (m, S, n, u, g), m and n are the wall reflection orders in the main street and the perpendicular street, respectively, $g = 0, 1$ is for the ground reflection, λ is the wavelength, k is the wave number, $\Re^i_{V,H}$, $R^{im}_{H,V}$ and $R^{in}_{H,V}$ are the well-known Fresnel reflection coefficients for ground and wall reflections in the main and perpendicular streets, respectively, with transmission in vertical, horizontal polarization, respectively. Also, with the notation shown in Figure 1, $S = 1$, (2) for BS images with first reflection on the wall $-y_1$ and $(w_1 - y_1)$, respectively, and $u = 1$, (2) for MS images with first reflection order on the wall $x - x_1$, and

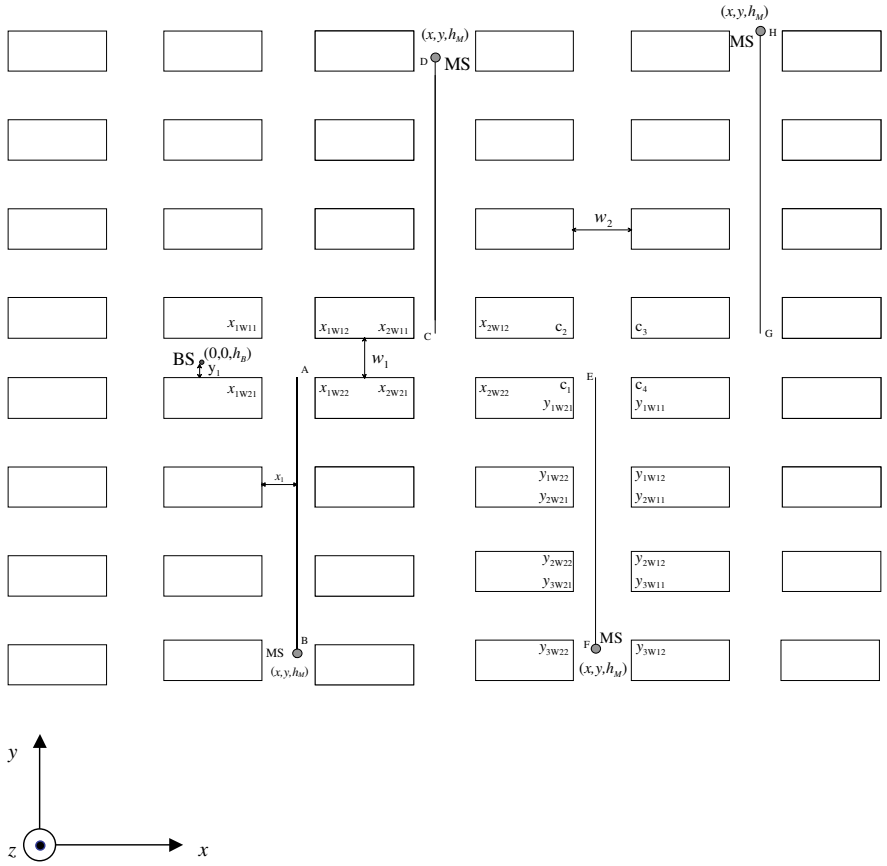

Figure 1. Urban street grid showing perpendicular street and crossing corners information. Studied traveling routes *A*-*B*, *C*-*D*, *E*-*F*, and *G*-*H* are shown.

$(x - x_1 + w_2)$ respectively. The $f_B(\theta, \phi)$ and $f_M(\Theta, \Phi)$ are the base station (BS) and the mobile station (MS) antenna field patterns with polarization information, respectively. The angles (θ, Θ) and (ϕ, Φ) are the elevation and azimuth angles for BS and MS, respectively, and (θ_i, Θ_i) and (ϕ_i, Φ_i) are the ray i corresponding angles. The following definition is adapted for the angles θ, Θ, ϕ and Φ: the angles θ and Θ equal to zero indicate the vertical directions at the BS and MS locations, respectively, and the angles ϕ, Φ equal to zero indicate the x-axis directions both the BS and MS, respectively. In (2), when m, n, g are zeros, the ray i is the direct path between transmitting and receiving antennas. Its counterpart ground reflection ray is obtained

by setting $g = 1$ while m and n are zeros.

Since calculation of both phase and amplitude of $H_{V,H}$ requires path lengths of the rays, an explicit form is derived by using image theory. The use of image theory determines the exact specular reflection point. It enables to identify which images would contribute to the received signal. This work presents horizontal plane angle set membership criterion to find the rays that couple the transmitter to the receiver from those that do not enter the perpendicular street or are lost in other streets before they arrive to the receiver. For a mobile station located at (x, y, h_M), the path length of the ray i with m and n reflection orders in the main and the perpendicular streets, respectively, is written as:

$$r_i = \sqrt{\begin{array}{l}((n+(-1)^u\Xi(n))w_2+(-1)^u(x-2\Xi(n)x_1))^2 \\ \quad +\left((-1)^S\left(\left(m+(-1)^S\Xi(m)\right)w_1-2(-1)^S\Xi(m)y_1\right)-y\right)^2 \\ \quad\quad +(h_B-(-1)^g h_M)^2\end{array}} \tag{3}$$

where

$$\Xi(\chi) = \begin{cases} 0, & \forall\ \chi \text{ even} \\ 1, & \forall\ \chi \text{ odd}, \end{cases} \tag{4}$$

h_B, h_M are the BS and the MS antenna heights, respectively, w_1 and w_2 are widths of the main and perpendicular streets, x_1 and y_1 are the distances shown on Figure 1. The angular information required for antenna field pattern and the potential use of adaptive antenna arrays [17] can be obtained from the environment geometry. The elevation angles of the ray i at the BS and the MS are given by

$$\theta_i = (1-g)\pi - (-1)^g\Theta_i = \frac{\pi}{2} + \arcsin\left(\frac{h_B-(-1)^g h_M}{r_i}\right) \tag{5}$$

The azimuth angles of the ray i at the BS and the MS are given by

$$\phi_i = \arctan\left(\frac{(-1)^m \text{sgn}(y)\left((m-\text{sgn}(y)\Xi(m))\,w_1+2\text{sgn}(y)\Xi(m)y_1+|y|\right)}{(-1)^u\left((n+(-1)^u\Xi(n))\,w_2+(-1)^u(x-2\Xi(n)x_1)\right)}\right) \tag{6}$$

$$\Phi_i = \arctan\left(\frac{(-1)^S((m+(-1)^S\Xi(m))w_1-2(-1)^S\Xi(m)y_1)-y}{(-1)^{(n+1)}\left((-1)^u((n+\Xi(n))\,w_2-2\Xi(n)x_1)+x\right)}\right) \tag{7}$$

where arctan $(\cdot)$ returns the angle in the corresponding quadrant.

The reflection loss can be calculated with the plane wave Fresnel reflection coefficient. The Fresnel reflection coefficient $\Re^i_{V,H}$ of

vertically and horizontally polarized waves for ground reflections is written as

$$\Re^i_{V,H} = \frac{\cos\gamma_i - a_{V,H}\sqrt{\varepsilon - \sin^2\gamma_i}}{\cos\gamma_i + a_{V,H}\sqrt{\varepsilon - \sin^2\gamma_i}} \tag{8}$$

where $a_V = 1/\varepsilon$ and $a_H = 1$ correspond to $\Re^i_V$ and $\Re^i_H$, respectively, $\varepsilon = \varepsilon_r - j60\lambda\sigma$. The reflection angle γ_i needed to calculate the ground reflection $\Re^i_{V,H}$ is given by

$$\gamma_i = \arctan\left(\frac{\sqrt{\begin{array}{l}((n+(-1)^u\Xi(n))w_2 + (-1)^u(x-2\Xi(n)x_1))^2 \\ +((-1)^S((m+(-1)^S\Xi(m))w_1 - 2(-1)^S\Xi(m)y_1) - y)^2\end{array}}}{(h_B + h_M)}\right) \tag{9}$$

For vertically, horizontally polarized antennas, the electric field would be horizontally, vertically polarized with respect to wall. In (2) $R^i_{H,V}$, the wall Fresnel reflection coefficient, can be calculated by (8) provided that ground reflection angle (γ_i) is replaced by the wall reflection angle (α_i). The reflection angle of the ray i in the main street (α_{im}) and in perpendicular street is (α_{ip}) needed to calculate the wall reflection $R^i_{H,V}$, are derived as

$$\alpha_{im} = \arctan\left(\frac{\sqrt{\begin{array}{c}((n+(-1)^u\Xi(n))w_2 + (-1)^u(x-2\Xi(n)x_1))^2 \\ +(h_B - (-1)^g h_M)^2\end{array}}}{\left|\begin{array}{l}(-1)^S((m+(-1)^S\Xi(m))w_1 \\ \quad -2(-1)^S\Xi(m)y_1) - y)\end{array}\right|}\right) \tag{10}$$

and

$$\alpha_{ip} = \arctan\left(\frac{\sqrt{\begin{array}{l}((-1)^S((m+(-1)^S\Xi(m))w_1 \\ -2(-1)^S\Xi(m)y_1) - y)^2 + (h_B - (-1)^g h_M)^2\end{array}}}{\left|\begin{array}{l}(n+(-1)^u\Xi(n))w_2 \\ \quad +(-1)^u(x - 2(-1)^u\Xi(n)x_1)\end{array}\right|}\right) \tag{11}$$

A. Determination of R-R Coupling Rays

In order to check for rays that couple the BS to the MS, a set of angles in the horizontal plane are used to utilize set membership criteria

to determine the coupling rays. The checking criterion first determines the set of angles correspond to rays that may enter the perpendicular street. Then, it determines the set of angles that correspond to rays that are lost in either side street before the perpendicular street or the rays that are lost in one of the parallel streets branched from the perpendicular street before they reach the mobile. In order to check for rays that enter to the perpendicular street, the horizontal plane angle of the ray i given by

$$\alpha_{i\_hplane} = \arctan\left(\frac{y-(-1)^S((m+(-1)^S\Xi(m))w_1-2(-1)^S\Xi(m)y_1)}{(-1)^u((n+(-1)^u\Xi(n))w_2+(-1)^u(x-2\Xi(n)x_1))}\right) \tag{12}$$

must satisfy the following set membership criteria:

$$\alpha_{i\_hplane} \in \left\{ \begin{array}{ll} \alpha : \alpha_{i\_lthr} < \alpha < \alpha_{i\_uthr} \cap \alpha \underset{S=2}{\overset{S=1}{\gtrless}} \alpha_{i\_c\eta}, & \forall m > 0 \\ \alpha : \alpha_{i\_lthr} < \alpha < \alpha_{i\_uthr}, & m = 0 \end{array} \right\} \tag{13}$$

where

$$\alpha_{i\_(uthr,lthr,c\eta)} = \arctan\left(\frac{y_{c(\mu,\beta,\eta)} - (-1)^S((m+(-1)^S\Xi(m))w_1 - 2(-1)^S\Xi(m)y_1)}{x_{c(\mu,\beta,\eta)}}\right) \tag{14}$$

where $(x_{c_i}, y_{c_i})_{i=1\,to\,4}$ are the positions of the corners at the crossing streets between the BS and the MS street, the subscripts $\mu = 4$, (2) , $\beta = 1$, (3) and $\eta = 2$, (1) are selected based on $S = 2$, (1), respectively.

Once the first set membership testing approves that the ray may enter the perpendicular street, it is necessary to check that the ray does not belong to rays that travel in any side street before the perpendicular street where the MS is located. The horizontal plane angle α_{i_hplane} of the ray that does not travel into the side streets before the perpendicular street must satisfy the set membership criterion given as

$$\alpha_{i\_hplane} \notin \bigcup_{p=1}^{J} \bigcup_{Q=\min(\aleph)}^{\max(\aleph)} \left\{ \alpha : \alpha_{pWGmQ\ 1} \underset{S=1}{\overset{S=2}{\lessgtr}} \alpha \underset{S=1}{\overset{S=2}{\lessgtr}} \alpha_{pWGmQ\ 2} \right\} \tag{15}$$

where

$$\alpha_{pWGmQ\xi} = \arctan\left(\frac{(-1)^S Q w_1 - y_1 - (-1)^S((m+(-1)^S \Xi(m))w_1 - 2(-1)^S \Xi(m) y_1)}{x_{pWG\xi}}\right) \tag{16}$$

$$\aleph = [1, 2 \ldots m] - \Xi(S) \tag{17}$$

where $p = 1, 2, \ldots, j$ (i.e., crossing streets before perpendicular street $1, 2, \ldots,$ upto j), $\xi = 1, 2$, $G = S - (-1)^S \Xi(Q)$ and $x_{pWG\xi}$ is the position of a corner of a crossing street p (see Fig. 1). The upper and lower bound in (15) determine rays that enter the side streets before the perpendicular street. Once the ray is determined to enter the perpendicular street, the last examination is to check that it does not travel to parallel street branched from the perpendicular street. Thus, the horizontal plane angle α_{i_hplane} of the ray i in the perpendicular street must satisfy the following set membership criterion

$$\alpha_{i\_hplane} \notin \bigcup_{a=1}^{L} \bigcup_{v=1}^{n} \{\alpha : \alpha_{aWAmv2} < \alpha < \alpha_{aWAmv1}\} \tag{18}$$

where

$$\alpha_{aWAmv\xi} = \arctan\left(\frac{y_{aWA\zeta} - (-1)^S((m + (-1)^S \Xi(m))w_1 - 2(-1)^S \Xi(m) y_1)}{(-1)^u (v w_2 - x_1) + x}\right) \tag{19}$$

where $a = 1, 2, \ldots, L$ (i.e., parallel streets $1, 2, \ldots,$ up to L branched from perpendicular street but before the location of the MS), $\xi = 1, 2$, $A = u - (-1)^u \Xi(v)$, and $y_{aWA\xi}$ is the position of a certain crossing street corner (see Fig. 1).

2.1.2. Reflection-Diffraction-Reflection Rays

Building corners have an important role in diverting signals in to perpendicular streets. Diffraction at each corner of the street intersection contributes to the total received signal. The channel transfer function of rays that results from diffraction at the four building corners is

$$H_{RDR} = H_{C1} + H_{C2} + H_{C3} + H_{C4} \tag{20}$$

where $H_{C\ell}$ is the transfer function of the rays experiencing diffraction at corner ℓ. The electric field for a ray generated from the diffraction process on the building corner is calculated by applying the uniform geometrical theory of diffraction. The UTD approach considers a single ray at a time and piece together an overall received signal as a sum of all the diffracted rays. The channel transfer function [14] of rays experiencing reflection-diffraction-reflection phenomena before the receiving antenna can be calculated by

$$H_{V,H} = \left(\frac{\lambda}{4\pi}\right)_{ray} \sum_{i\equiv(m,S,n,u,g,C_i)} \Bigg[f_B(\theta_i,\phi_i) f_M(\Theta_i,\Phi_i) \left(\Re^i_{V,H}\right)^g \left(R^{im}_{H,V}\right)^m \mathcal{D}^i_{H,V} \left(R^{in}_{iH,iV}\right)^n \frac{1}{\sqrt{D_1 D_2 (D_1+D_2)}} e^{-jk(D_1+D_2)} \Bigg] \quad (21)$$

where $\mathcal{D}^i_{H,V}$ is the UTD diffraction coefficient at the vertical edge of the building corner, $D_{1,2}$ is the distances from the BS and the MS to the diffraction point, respectively. These are defined as follows:

$$D_{1,2} = \sqrt{d^2_{1,2} + (h_{B,M} - H_{corner})^2} \quad (22)$$

where H_{corner} is the diffraction point height at the building corner, d_1 and d_2 are the horizontal plane distances from the BS and the MS to the diffracting corner, respectively, which are defined as

$$H_{corner} = \begin{cases} \dfrac{d_2 h_B + (-1)^g d_1 h_M}{d_1 + d_2}, & \forall\ d_2 h_B > d_1 h_M \\ \dfrac{(-1)^g d_2 h_B + d_1 h_M}{d_1 + d_2}, & \forall\ d_2 h_B < d_1 h_M \end{cases} \quad (23)$$

$$d_1 = \sqrt{X_c^2 + ((-1)^S((m + (-1)^S \Xi(m))w_1 - 2(-1)^S \Xi(m) y_1) - Y_c)^2} \quad (24)$$

$$d_2 = \sqrt{\begin{array}{c}(y - Y_c)^2 + ((-1)^u((n + (-1)^u \Xi(n))w_2 \\ +(-1)^u(x - 2\Xi(n)x_1)) - X_c)^2\end{array}} \quad (25)$$

where $S = 1$, (2) for H_{c2} and H_{c3}, (H_{c1} and H_{c4}), respectively and $u = 2$ (1) for H_{c1} and H_{c2}, (H_{c3} and H_{c4}), respectively, and X_c and Y_c are co-ordinates of corner c_l. In (23) the switching between the two equations is based on whether the ground reflection takes place after or before diffraction.

A. Determination of R-D-R Coupling Rays

In order to determine the set of rays that connect the two terminals, a set of membership criterion must be fulfilled. Coupling rays having certain angular ranges can propagate from the main street in to the perpendicular street. In this work, the coupling rays from other side streets to parallel street and back to the perpendicular street are neglected. They are assumed to experience high attenuation due to double diffraction and they are much less likely to occur with significant power. The coupling radio paths have angular characteristics that must fulfill set membership criteria. They must not belong to rays propagate in other side streets before the perpendicular street. Moreover, the perpendicular street junction corners divert those rays having angular characteristics that make them to propagate in the perpendicular street. Furthermore, to ensure that the ray reaches the MS, it must have angular characteristics that exclude it from rays that propagate in parallel streets branched from the perpendicular street before the location of the MS. In order to study these angular characteristics, horizontal plane angle of each ray in both the main and perpendicular streets are used to check if the ray belongs to rays having certain set of angles. The horizontal plane angle of ray i in the main street is given by

$$\alpha_{ihp\_m} = \arctan\left(\frac{(-1)^S((m+(-1)^S\Xi(m))w_1 - 2(-1)^S\Xi(m)y_1 - Y_c)}{-X_c}\right) \tag{26}$$

Thus, three sets of angle membership criteria must be examined to check for coupling radio paths. First test is to ensure that the ray does not propagate in the side streets before the perpendicular street. To satisfy this condition, the following criterion must be fulfilled for each corner (H_{c1}-H_{c4}),

$$\alpha_{ihp\_m} \notin \bigcup_{p=1}^{J}\bigcup_{q=1}^{m}\left\{\alpha : \alpha_{m\_pWGq2} \underset{c2,c3}{\overset{c1,c4}{\leqslant}} \alpha \underset{c2,c3}{\overset{c1,c4}{\leqslant}} \alpha_{m\_pWGq1}\right\} \tag{27}$$

where

$$\alpha_{m\_pWGq\xi} = \arctan\left(\frac{(-1)^S q w_1}{x_{pWG\xi} - X_c}\right) \tag{28}$$

where $p = 1, 2, \ldots, J$ (i.e., crossing streets before perpendicular street $1, 2, \ldots,$ upto J), $\xi = 1, 2$, $G = S - (-1)^S\Xi(q)$ and $x_{pWG\xi}$ is the position of a certain crossing street corner (see Fig. 1). The upper and lower bound in (27) determine rays that enter the side streets

and are neglected as explained earlier. Once the ray is determined not to propagate into one of the side streets before the perpendicular street, the second examination is to check whether the concerned corner (c_1, c_2, c_3 or c_4) diverts the signal into the perpendicular street. First, the direct and multiple reflection rays from the BS that illuminate each corner are determined. Then, determining the set of rays that each illuminated corner diverts in to the perpendicular street. The rays that couple the BS and its images to each illuminated corner must satisfy the angular criterion

$$\alpha_{ihp\_m} \in \left\{ \alpha : \alpha \underset{\substack{l=2,3\\k=1,1}}{\overset{\substack{l=1,4\\k=2,2}}{\gtrless}} \alpha_{c_1-c_k} \right\} \tag{29}$$

$$\alpha_{c_l-c_k} = \arctan\left(\frac{y_{c_k}-y_{c_l}}{x_{c_k}-x_{c_l}}\right) \tag{30}$$

where(x_{c_l}, y_{c_l}), (x_{c_k}, y_{c_k}) are the co-ordinates of the lth or kth corners of the perpendicular streets, and the rays that are diverted from corner l and propagate to the side street must satisfy the following criterion:

$$\alpha_{ihp\_s} \in \left\{ \begin{array}{l} \alpha : \alpha \underset{\substack{l=1,2\\k=4,4}}{\overset{\substack{l=3,4\\k=1,1}}{\gtrless}} \alpha_{c_1-c_k}, \quad \forall\ y < y_1 \\ \alpha : \alpha \underset{\substack{l=3,4\\k=2,2}}{\overset{\substack{l=1,2\\k=3,3}}{\gtrless}} \alpha_{c_1-c_k}, \quad \forall\ y > (w_1 - y_1) \end{array} \right\} \tag{31}$$

where α_{ihp_s} is the horizontal plane angle of the propagating ray in perpendicular street which is utilized to check the set membership criterion. The horizontal plane angle is defined as

$$\alpha_{is\_hp} = \arctan\left(\frac{y - Y_c}{((-1)^u((n+(-1)^u \Xi(n))w_2 + (-1)^u(x - 2\Xi(n)x_1)) - X_c)}\right) \tag{32}$$

Once the ray has been determined to propagate to the perpendicular street, the last check is to test that the ray does not propagate to the parallel streets branched from the perpendicular street before the MS. The rays that couple the illuminated corner with

the MS must satisfy the following set membership criterion:

$$\alpha_{is-hp} \notin \bigcup_{a=1}^{L} \bigcup_{b=1}^{n} \left\{ \begin{array}{l} \alpha : \alpha_{s-aWAb1} \underset{c3,c4}{\overset{c1,c2}{\leqslant}} \alpha \underset{c3,c4}{\overset{c1,c2}{\leqslant}} \alpha_{s-aWAb2}, \\ \qquad\qquad\qquad \forall\ y \leq y_1 \\ \alpha : \alpha_{s-aWAb1} \underset{c3,c4}{\overset{c1,c2}{\geqslant}} \alpha \underset{c3,c4}{\overset{c1,c2}{\geqslant}} \alpha_{s-aWAb2}, \\ \qquad\qquad\qquad \forall\ y \geq (w_1 - y_1) \end{array} \right\} \quad (33)$$

where

$$\alpha_{s\_aWAb} = \operatorname{atan}\left(\frac{y_{aWA\xi} - Y_c}{(-1)^u b w_2}\right) \quad (34)$$

where $a = 1, 2, \ldots, L$ (i.e., crossing streets before perpendicular street $1, 2, \ldots$, upto L), $\xi = 1, 2$, $A = u - (-1)^u \Xi(b+1)$ and $y_{aWA\xi}$ is the position of a certain crossing street corner (see Fig. 1). The upper and lower bound in (33) determine rays that enter the parallel streets before the MS.

Once the ray is determined to couple the BS station to the MS, the calculation of the transfer function (21) gives the characteristics of the channel. The angular information needed for antenna field pattern and the potential use of adaptive antenna arrays [17] can be obtained from environment geometry. The elevation angles of the ray i at the BS and the MS are given by

$$\theta_i = (1-g)\pi - (-1)^g \Theta_i = \frac{\pi}{2} + \arcsin\left(\frac{(h_B - (-1)^g h_M)}{(D_1 + D_2)}\right) \quad (35)$$

$$\phi_i = \arctan\left(\frac{(-1)^{S+m+1}((m + \Xi(m))w_1) + Y_c}{X_c}\right) \quad (36)$$

$$\Phi_i = \arctan\left(\frac{(Y_c - y)}{(-1)^{u+n+1}((n + \Xi(n))w_2) + X_c - x}\right) \quad (37)$$

B. Diffraction Coefficient

The UTD diffraction coefficient ($\mathcal{D}^i_{H,V}$) is necessary to calculate the amplitude and phase of each ray. The choice of the diffraction coefficient is important for accurately predicting the signal amplitude resulted from the diffraction process. Diffraction formulas are well established for perfectly conducting (PC) infinite wedges [3, 4], for absorbing wedges [18], and for impedance-surface wedges [19, 20]. However, many important applications, such as in mobile

communications, involve large dielectric structures. In these cases, the assumption of PC boundary conditions results in a lack of accuracy in predicting the actual electromagnetic field. On the other hand, the impedance-surface diffraction formulas are rather cumbersome to use in routine applications such as propagation prediction tools in mobile communications due to their complexity. Thus, from the point of view of engineering applications, the difficulty of using the rigorous solutions for propagation prediction forces simplifications to be made. Some existing diffraction coefficients [5, 21, 22] modify the PC-UTD diffraction coefficient in order to make it applicable to dielectric wedges. For a normal incident plane wave, we present a general form of the PC-UTD-based diffraction coefficient that makes existing PC-UTD- based solutions as special cases of it. The general form can be expressed as:

$$\mathcal{D}^i_{H,V} = \Gamma_1 D^{(1)} + \Gamma_2 D^{(2)} + \Gamma_3 D^{(3)} + \Gamma_4 D^{(4)} \tag{38}$$

The components $D^{(l)}(l = 1, 2, 3, 4)$ of the diffraction coefficient in (38) are given by [21]

$$D^{(l)} = \frac{-e^{-j\pi/4}}{2n\sqrt{2\pi k}} \cot\gamma^{(l)} F_o\left(2kLn^2 \sin^2\gamma^{(l)}\right) \tag{39}$$

where $n\pi$ is the exterior angle of the wedge; F_o is the transition function, $\gamma^{(1)} = [\pi - (\phi - \phi')]/2n$, $\gamma^{(2)} = [\pi + (\phi - \phi')]/2n$, $\gamma^{(3)} = [\pi - (\phi + \phi')]/2n$, $\gamma^{(4)} = [\pi + (\phi + \phi')]/2n$, n is related to wedge angle Ψ, ϕ' and ϕ are the incidence and the diffraction angles. Detailed descriptions of the variables that appear in (39) are given in [3–5]. The angle ϕ' and ϕ needed for calculation of $\mathcal{D}^i_{H,V}$ in (21) can be calculated from the horizontal plane ray angles in the main and the perpendicular streets as

$$\phi' = \begin{cases} \pi - \alpha_{ihp\_m}, & \text{for corner } C_1 \\ \alpha_{ihp\_m} - \pi, & \text{for corner } C_2 \\ \alpha_{ihp\_m} - 0.5\pi, & \text{for corner } C_3 \\ 1.5\pi - \alpha_{ihp\_m}, & \text{for corner } C_4 \end{cases} \tag{40}$$

and

$$\phi = \begin{cases} \pi - (\text{sgn}(y) - 1)\pi - \alpha_{ihp\_s}, & \text{for corner } C_1 \\ \pi + (\text{sgn}(y) - 1)\pi + \alpha_{ihp\_s}, & \text{for corner } C_2 \\ \alpha_{ihp\_s} - 0.5\pi, & \text{for corner } C_3 \\ 1.5\pi - \alpha_{ihp\_s}, & \text{for corner } C_4 \end{cases} \tag{41}$$

Different definitions of multiplication factors Γ_i $(i = 1, \ldots, 4)$ of each term in (38) result in different diffraction coefficients that

appear in literature. For $\Gamma_{1,2,3,4} = 1$, and $\Gamma_{1,2} = 1$, $\Gamma_{3,4} = -1$ we obtain the PC-UTD diffraction coefficient for perpendicular and parallel polarizations [3, 4], respectively. For a vertically polarized transmitting antenna, the electric field is in parallel to vertical edges at the building corners. In [5], Luebbers kept $\Gamma_{1,2} = 1$ and heuristically set $\Gamma_{3,4} = R_{0,n}^{\parallel,\perp}$, where $R_{0,n}^{\parallel,\perp}$ is the plane wave Fresnel reflection coefficient for o-face (i.e., $\phi = 0$) and n-face (i.e., $\phi = n\pi$) of the wedge with parallel ($\parallel$) and perpendicular ($\perp$) polarizations. He conjectured that this approach would yield a reliable estimate for the diffraction coefficient, particularly, around the incidence and reflection shadow boundaries. Furthermore, Holm in [21] heuristically modified the PC-UTD diffraction coefficient by changing the factors $\Gamma_{1,2}$ and keeping the modification introduced by Luebbers for $\Gamma_{3,4}$. In particular, when the source illuminates the o-face, Holm set $\Gamma_1 = R_0^{\parallel,\perp} \cdot R_n^{\parallel,\perp}$ and kept $\Gamma_2 = 1$ and when the source illuminates the n-face, he modified $\Gamma_2 = R_0^{\parallel,\perp} \cdot R_n^{\parallel,\perp}$ and kept $\Gamma_1 = 1$ with some changes in the definition of the reflection angle. In [22], a new definition of Γ_l is proposed. It uses a modified reflection coefficient that is inferred from a suitable formulation of the Maliuzhinets solution [19, 20]. Another heuristic solution based on absorbing wedges diffraction coefficient which is proposed in [23] shows good agreement with measurements in microcellular environment.

3. NUMERICAL RESULTS

In mobile communications for urban microcellular environment, the base station antennas are placed below the surrounding buildings. The location and buildings structures have strong impact on the radio wave propagation characteristics and cell shape. In this section, a street grid environment found in many cities has been simulated for the calculations of the microcell propagation characteristics. The grid pattern has 100 m × 50 m blocks of buildings and 25 m street widths for the main, side and parallel streets. In the simulation results below, the carrier frequency is 2.154 GHz, the base and mobile station antenna heights are 13 m and 1.8 m, respectively. Omnidirectional antennas with vertical polarization are assumed. Following [6], electrical parameters $\sigma = 0.005$ and $\varepsilon_r = 15$ and $\varepsilon_r = 5$ are used when calculating ground and wall reflection loss, respectively. The simulated environment is shown in Figure 1. The BS is located at $y_1 = 5$ m and the MS travels along different routs with distance $x_1 = 13$ m from the wall (see Fig. 1). Different routes have been tested, namely, *A*-*B*, *C*-*D*, *E*-*F*, and *G*-*H* as shown in Figure 1. In order to have detailed

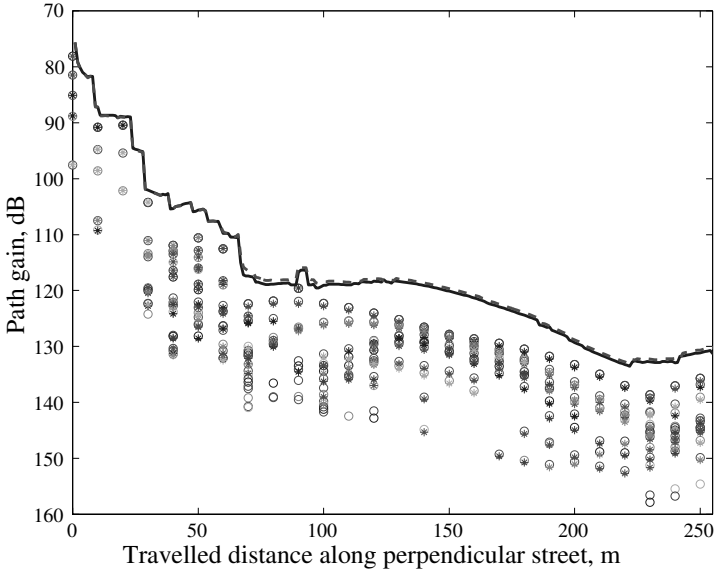
Path gain, dB
Travelled distance along perpendicular street, m
70
80
90
100
110
120
130
140
150
160
0
50
100
150
200
250

(a)

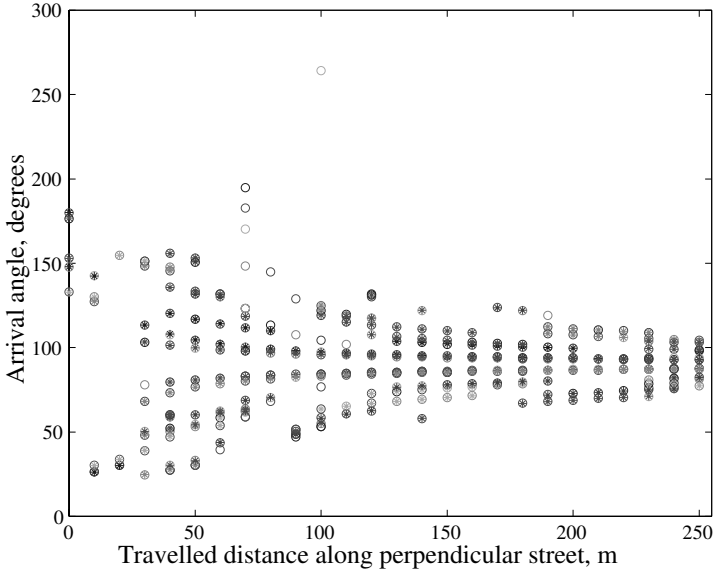
Arrival angle, degrees
Travelled distance along perpendicular street, m
300
250
200
150
100
50
0
0
50
100
150
200
250

(b)

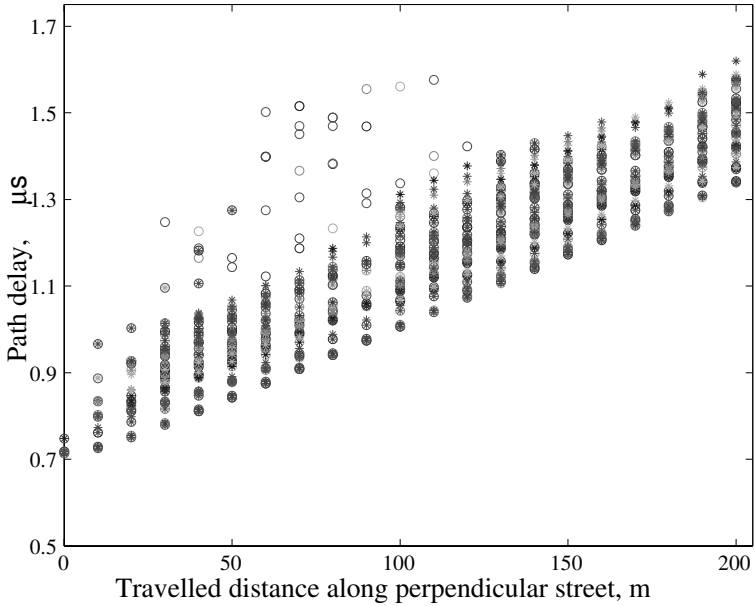

(c)

Figure 2. Propagation characteristics in route *A*-*B*. (a) Path gain. (b) Rays angle of arrival at the mobile station. (c) Rays path delays.

characterization of the multipath channel, each path is characterized in terms of its power, delay and angular information. In order to validate the proposed model, the results of this work are compared to simulation results obtained from a ray tracing algorithm based on vertical plane launch (VPL) [6] approach. The vertical plane launch (VPL) method is a robust three-dimensional ray tracing technique that can compute the multiple arriving rays in a heterogeneous building environment for base-station antennas located at any height. The VPL approach accounts for specular reflections from vertical building surfaces and diffraction at vertical edges and approximates diffraction at horizontal edges by restricting the diffracted rays to lie in the plane of incidence, or in the plane of reflection. The diffraction coefficient presented in [23] is used in later numerical computations both in the proposed model and the VPL algorithm. The comparison is made in gain, angular and path delay information of coupling rays. In order to have clear presentation of the comparison results of individual ray characteristics, the comparison is made in steps of 10 m. In all figures, the circles ('O') represent VPL simulation results and the stars ('*')

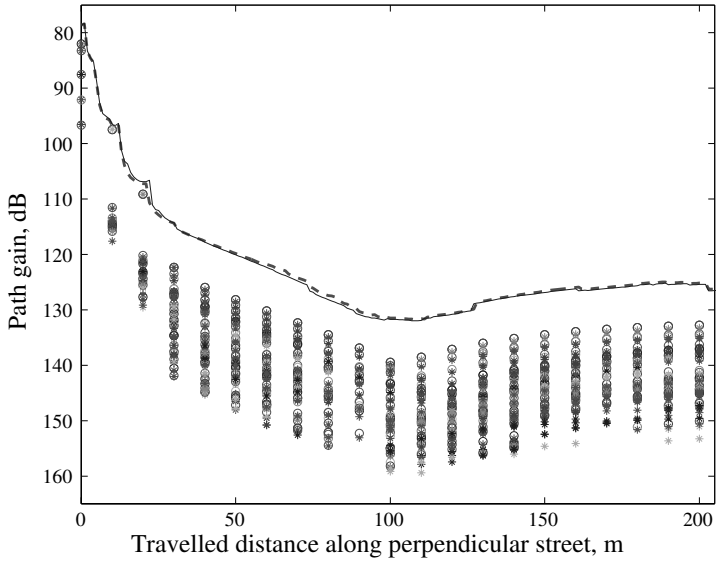
Path gain, dB
80
90
100
110
120
130
140
150
160
0
50
100
150
200
Travelled distance along perpendicular street, m

(a)

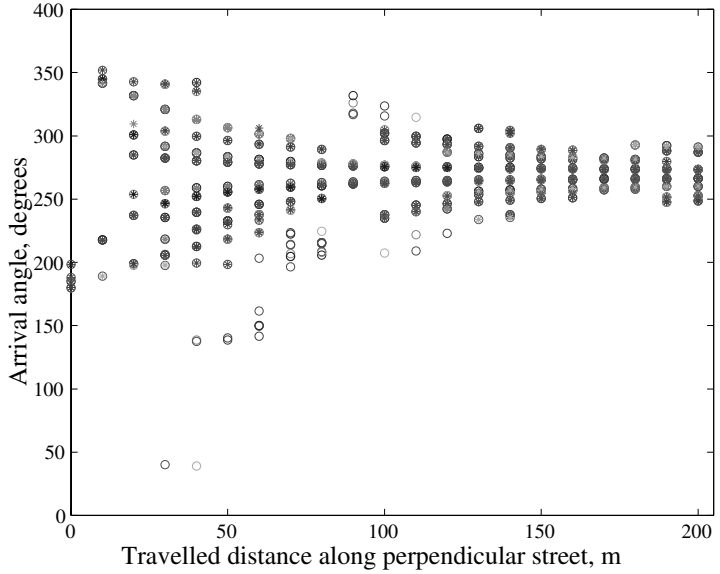
Arrival angle, degrees
400
350
300
250
200
150
100
50
0
0
50
100
150
200
Travelled distance along perpendicular street, m

(b)

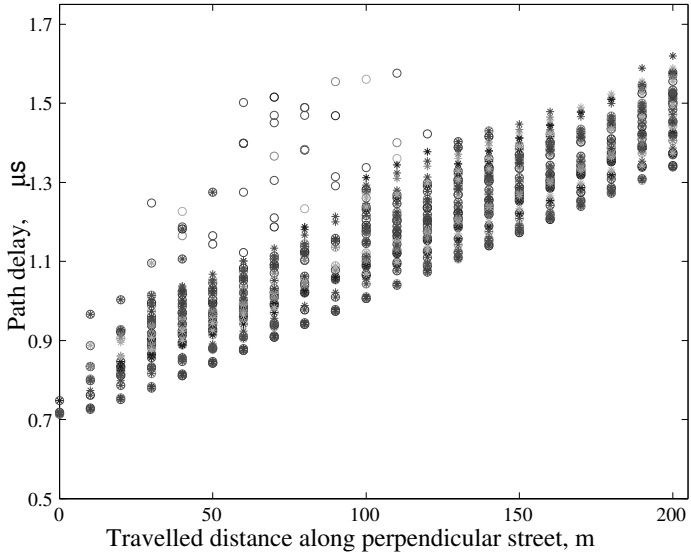

(c)

Figure 3. Propagation characteristics in route *C*-*D*. (a) Path gain. (b) Rays angle of arrival at the mobile station. (c) Rays path delays.

represent the proposed model results. Each 'O' and '*' represent one ray from VPL or this work model, respectively. The total number of 'O' or '*' in one MS location is the number of coupling rays at that location. Different combinations of reflection orders with and without diffraction have been tested. In all presented results, rays whose power is at least 20 dB below the strongest path are dropped out. Figure 2 shows comparison results for route *A*-*B*. The comparison is made for both groups of rays, the *R*-*R* and the *R*-*D*-*R* rays. The reflection order of up to 7 for *R*-*R* rays and the *R*-*D*-*R* rays has no reflection before diffraction but up to 5 reflection orders after diffraction has been tested for comparison. Figure 2(a) shows comparison results of the total power of all rays and power of each path found by the proposed model and the VPL. The solid and dashed lines represent the total power calculated by model in presented this work and the VPL solution, respectively. The figure shows clear agreement between the proposed model and VPL solution. This validates the assumption of the proposed model that the main energy in the perpendicular street comes via coupling of energy from the main street to the perpendicular street via the crossing junction. However, the VPL shows a few rays coming from radio paths coupled from the side streets to the parallel

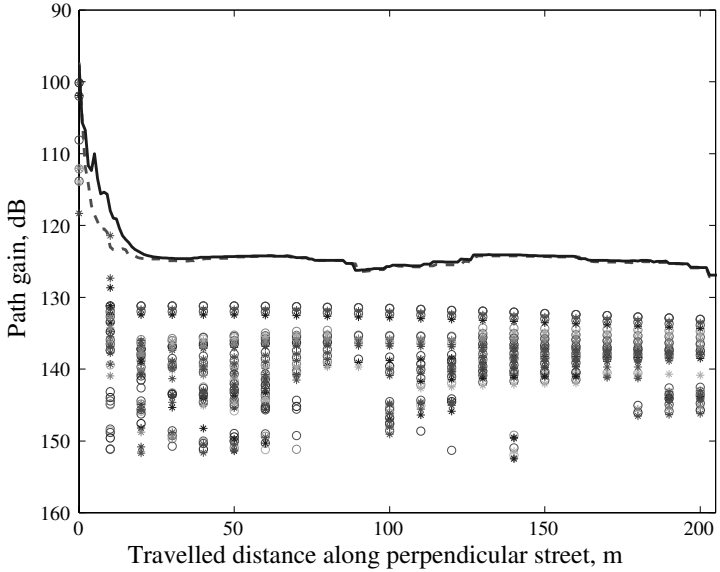
Path gain, dB
Travelled distance along perpendicular street, m
90
100
110
120
130
140
150
160
0
50
100
150
200

(a)

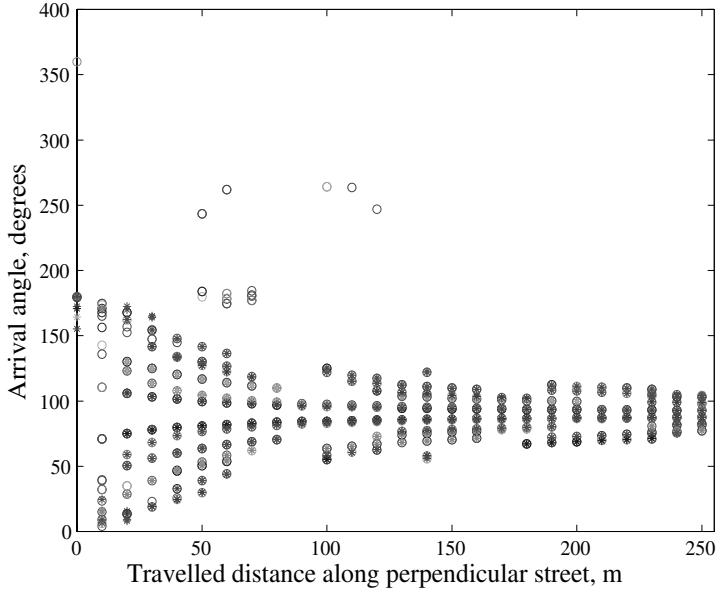
Arrival angle, degrees
Travelled distance along perpendicular street, m
400
350
300
250
200
150
100
50
0
0
50
100
150
200
250

(b)

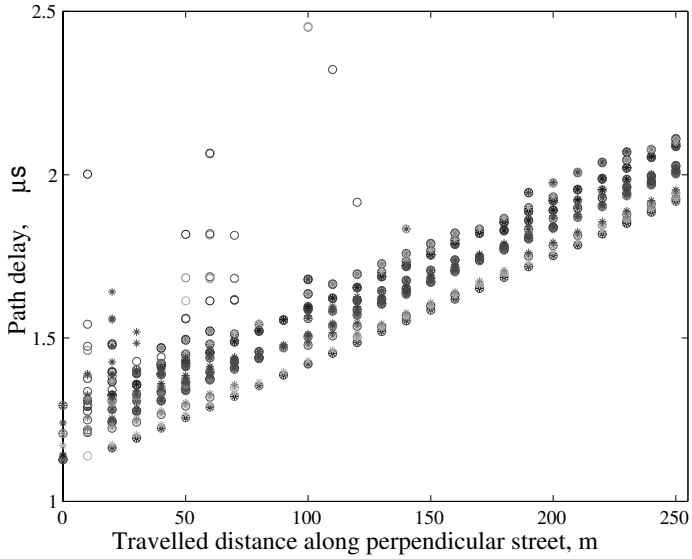

(c)

Figure 4. Propagation characteristics in route E-F. (a) Path gain. (b) Rays angle of arrival at the mobile station. (c) Rays path delays.

streets and back to the perpendicular streets. Due to their long path and many interactions, such rays have low power and in the whole route these events are rare to take place, which agrees with our assumption to ignore them. The powers of these rays are shown as the empty circles ('O') in Figure 2(a). Figure 2(b) shows comparison results in terms of azimuthal angular information of every path at the MS. The 0° is the x-axis direction. So, the route A-B and the assumption of coupling energy from the street junction shows that the main energy comes around 90°. It is clear that angular spread is large near the junction where both group of rays exist but the angular spread decreases as the MS travels down the street where only the components diffracted from building corners exist. The rays mentioned earlier, which couple via parallel streets, can be clearly seen in this figure as the rays of empty 'O'. Their arrival of direction opposite to that of the main energy is shown by the arrival angles at the MS, which indicate that they have traveled via other streets. These rays have also long delay due to their longer path compared to the main energy paths. These long delays are shown in Figure 2(c), presenting comparison results of each path delay. Clear agreement can be seen. The VPL rays,

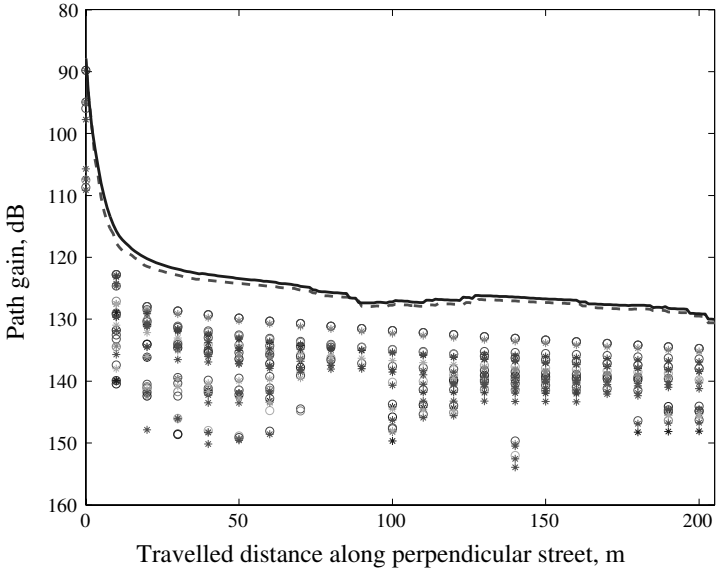
Path gain, dB
80
90
100
110
120
130
140
150
160
0
50
100
150
200
Travelled distance along perpendicular street, m

(a)

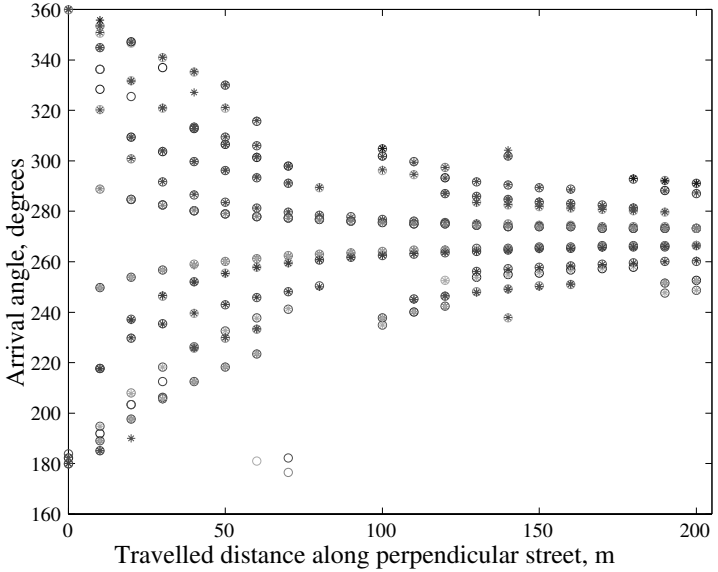
Arrival angle, degrees
360
340
320
300
280
260
240
220
200
180
160
0
50
100
150
200
Travelled distance along perpendicular street, m

(b)

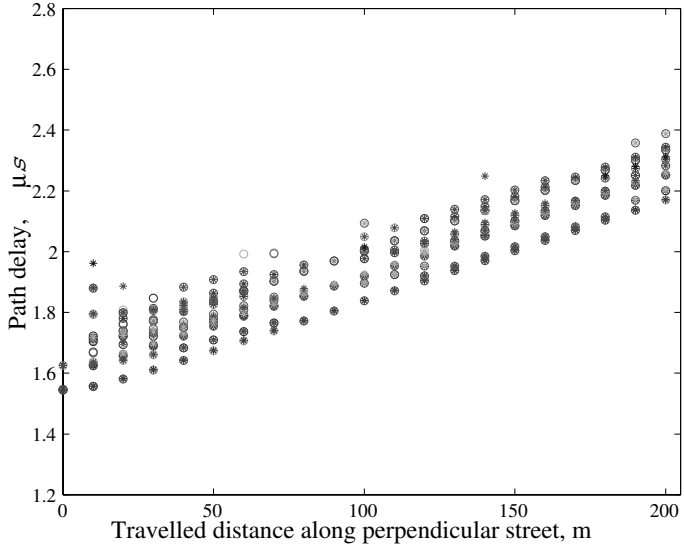

(c)

Figure 5. Propagation characteristics in route G-H. (a) Path gain. (b) Rays angle of arrival at the mobile station. (c) Rays path delays.

which have no corresponding rays given by the proposed model, are rays that experience reflection on the main street and may be on the perpendicular street but the diffraction takes place on the corners of the parallel street branched from the perpendicular street. They do not go over diffraction at the cross street junction corners (c_1–c_4). They also rarely take place. Figure 3 shows comparison results for route *C*-*D*. For this route, the reflection order of the *R*-*R* rays is kept 7 as in route *A*-*B* but the *R*-*D*-*R* ray group undergoes reflection up to 7 times before and after diffraction takes place are tested. Clear agreement for the total power and power, direction of arrival and delay of each ray is found between the results of the proposed model and the results obtained from the VPL simulation. Similar observation as that in route *A*-*B* concerning rays that arrive via parallel streets with low powers and long delays can be seen also for route *C*-*D*. Figures 4 and 5 show comparison results for routes *E*-*F* and *G*-*H*, respectively. In these scenarios, the perpendicular street visibility angle to the BS is very small. Thus, *R*-*R* rays are unlikely to couple the BS to the MS. For *R*-*D*-*R* rays, we tested one reflection order before diffraction and up to 5 reflections in the perpendicular street. Clear agreement can be seen and similar observation as stated earlier is noticed.

4. CONCLUSION

An explicit expression propagation model for perpendicular street of urban street grid for microcellular communication is proposed. The characterizing parameters of each propagation path are given in analytical forms. The proposed propagation model is validated with three-dimensional ray tracing technique. The proposed model is valid for perpendicular streets with any number of crossing streets between the base station the street of concern. The proposed model is easy to implement and fast in computation. As a result, the proposed propagation model can be used to study dispersion characteristics and other propagation problems in microcellular environments with applications in e.g., diversity techniques, MIMO capacity analysis, etc. As a future work, an explicit expression propagation model for parallel street is targeted to provide a comprehensive modeling approach together with the presented and previous [14] work.

REFERENCES

1. Dersch, U. and E. Zollinger, "Propagation mechanisms in microcell and indoor environment," *IEEE Trans. Antennas and Propagat.,* Vol. 43, 1058–1066, Nov. 1994.
2. Erceg, V., A. J. Rustako, and R. S. Roman, "Diffraction around corners and its effect on the microcell coverage area in urban and suburban environments at 900 MHz, 2 GHz, and 6 GHz," *IEEE Trans. Veh. Technol.,* Vol. 43, 762–766, Aug. 1994.
3. Kouyoumjian, R. G. and P. H. Pathk, "A uniform geometrical theory of diffraction for and edge in a perfectly conducting surface," *Proc. IEEE,* Vol. 62, 1448–1461, Nov. 1974.
4. McNamara, D. A., C. W. I. Pistorius, and J. A. G. Malherbe, *Introduction to the Uniform Geometrical Theory of Diffraction,* Artech House, Boston, London, 1996.
5. Luebbers, R. J., "Finite conductivity uniform UTD versus knife diffraction prediction of propagation path loss," *IEEE Trans. Antennas Propagat.,* Vol. AP-32, 70–76, Jan. 1984.
6. Liang, G. and H. Bertoni, "A new approach to 3-D ray tracing for propagation prediction in cities," *IEEE Trans. Antennas Propagat.,* Vol. AP-46, No. 6, 853–863, Jun. 1998.
7. Kanatas, A. G., I. D. Kounouris, G. B. Kostaras, and P. Constantinou, "A UTD propagation model in urban microcellular environments," *IEEE Trans. Veh. Technol.,* Vol. 46, 185–193, Jan. 1997.

8. Tan, S. Y. and H. S. Tan, "A microcellular communications propagation model based on the uniform theory of diffraction and multiple image theory," *IEEE Trans. Antennas and Propagat.,* Vol. 44, 1317–1326, Oct. 1996.
9. Liang, G. and H. L. Bertoni, "Review of ray modeling techniques for site specific propagation prediction," *Wireless Communications, TDMA Versus CDMA,* S. G. Glisic and P. A. Leppänen (eds.), 323-343, Kluwer Academic, Norwell, MA, 1997.
10. Athanasiadou, G. E., A. R. Nix, and J. P. McGeehan, "A microcellular ray tracing model and evaluation of its Narrow-band and wide-band predictions," *IEEE J. Select. Areas Commun.,* Vol. 18, No. 3, 322–355, March 2000.
11. Son, H.-W. and N.-H. Myung, "A deterministic ray tube method for microcellular wave propagation prediction model," *IEEE Trans. Antennas and Propagat.,* Vol. 47, 1344–1350, Aug. 1999.
12. Agelet, F. A., A. Formella, J. M. Hernando, F. I. de Vicente, and F. P. Fontan, "Efficient Ray-tracing acceleration techniques for radio propagation modeling," *IEEE Trans. Veh. Technol.,* Vol. 49, 2089–2094, Nov. 2000.
13. Rizk, K., J.-F. Wagen, and F. Gardiol, "Two-dimensional ray-tracing modeling for propagation in microcellular environments," *IEEE Trans. Veh. Technol.,* Vol. 46, 508–518, Feb. 1997.
14. El-Sallabi, H. and P. Vainiakainen, "Physical modeling of line-of-sight wideband propagation in a city street for microcellular communications," *Journal of Electromagnetic Waves and Applications,* Vol. 14, 904–927, 2000.
15. Foschini G. J. and M. Gans, "On the limits of wireless communications in fading environment when using multiple antennas," *Wireless Personal Communications,* Vol. 6, 311, March 1998.
16. Chizhik D., G. Foschini, M. Gans, and R. Valenzuela, "Keyholes, correlations and capacities of multi-element transmit and receive arrays," *Electronic letters,* Vol. 36, June 22, 2000.
17. Tsoulos, G. V. and G. E. Athanasiadou, "On the application of adaptive antennas to microcellular environments: radio channel characteristics and system performance," *IEEE Trans. Veh. Technol.,* Vol. 51, 1–16, Jan. 2002.
18. Felsen, L. B. and N. Marcuvitz, *Radiation and Scattering of Waves,* Prentice-Hall, Englewood Cliffs, NJ, 1973.
19. Maliuzhinets, G. D., "Excitation, reflection and emission of surface waves from a wedge with given face impedances," *Sov. Phys. Dokl.,* Vol. 3, No. 4, 752–755, 1958.

20. Tiberio, R., G. Pelosi, G. Manara, and P. H. Pathak, "High-frequency scattering from a wedge with impedance faces illuminated by a line source — Part I: Diffraction," *IEEE Trans. Antennas Propagat.,* Vol. 37, 212–218, Feb. 1989.
21. Holm, P. D., "A new heuristic UTD diffraction coefficient for nonperfectly conducting wedges," *IEEE Trans. Antennas Propagat.,* Vol. 48, 1211–1219, Aug. 2000.
22. El-Sallabi, H., I. T. Rekanos, and P. Vainiakainen, "A new heuristic diffraction coefficient for lossy dielectric wedges at normal incidence," *IEEE Antennas and Propagation Letters (AWPL)* Vol. 1, 165–168, 2002.
23. El-Sallabi, H. M., G. Liang, H. L. Bertoni, and P. Vainikainen, "Influence of diffraction coefficient and corner shape on ray prediction of power and delay spread in urban microcell," *IEEE Trans. on Antenna and Propag.,* Vol. 50, No. 5, 703–712, May 2002.